Multichannel scattering problem with a nonseparable angular part as a boundary-value problem

Shahpoor Saeidian[1,*] and Vladimir S. Melezhik[2,3,†]

[1]*Optics and Photonics Research Center, Department of Physics, Institute for Advanced Studies in Basic Sciences (IASBS), Gava Zang, Zanjan 45137-66731, Iran*

[2]*Bogoliubov Laboratory of Theoretical Physics, Joint Institute for Nuclear Research, Dubna, Moscow Region 141980, Russian Federation*

[3]*Peoples' Friendship University of Russia (RUDN University), 6 Miklukho-Maklaya Street, Moscow 117198, Russian Federation*

(Received 16 July 2017; revised manuscript received 12 September 2017; published 3 November 2017)

We have developed an efficient computational method for solving the quantum multichannel scattering problem with a nonseparable angular part. The use of the nondirect product discrete-variable representation, suggested and developed by V. Melezhik, gives us an accurate approximation for the angular part of the desired wave function and, eventually, for the scattering parameters. Subsequent reduction of the problem to the boundary-value problem with well-defined block-band matrix of equation coefficients permits us to use efficient standard algorithms for its solution. We demonstrate the numerical efficiency, flexibility, and good convergence of the computational scheme in a quantitative description of the Feshbach resonances in pair collisions occurring in atomic traps and the scattering in strongly anisotropic traps. The method can also be used for the investigation of further actual problems in quantum physics. A natural extension is a description of spin-orbit coupling, intensively investigated in ultracold gases, and dipolar confinement-induced resonances.

DOI: 10.1103/PhysRevE.96.053302

I. INTRODUCTION

Multichannel scattering arises in the description of different quantum processes in atomic and molecular physics, quantum chemistry, and nuclear physics. In recent years, multichannel scattering is of particular interest in the context of the accurate description of Feshbach resonances in ultracold gases [1,2]. The initial step of the conventional analysis of the scattering is to separate the angular part with the aid of expansion over spherical harmonics. However, in the case of strong coupling between the different partial waves, it can become questionable. Especially, the drawback of the partial-wave analysis is developed if the coupling remains non-negligible in the asymptotic region due to the long-range character of the interparticle interaction. Thus, in dipole-dipole scattering, occurring for example in atomic scattering in external laser field, the long-range term $\sim 1/r^3$ describing interatomic interaction leads to nonseparability of the partial scattering amplitudes even in the zero-energy limit [3]. In this case it is necessary to provide a special procedure for extracting the desired partial amplitudes [4]. An alternative approach without usual partial-wave analysis for treating scattering with a nonseparable angular part in the asymptotic region was suggested in the works of Melezhik [5] and Melezhik and Chi-Yu Hu [3]. Then, it was extended for multichannel scattering of cold atoms in quasi-one-dimensional harmonic traps [6] and successfully applied for a number of resonant processes in confined geometry of atomic traps [7–11]. The key element of the approach is to use, instead of the partial analysis, the nondirect product discrete-variable representation (npDVR) suggested and developed by Melezhik in a number of works [12–16].

In the present paper we describe the computational scheme, based on the npDVR, which we develop for multichannel confined scattering with a nonseparable angular part. We reformulate the scattering problem as a boundary-value problem for a system of algebraic equations with block-band structure of the well-defined matrix of coefficients which arises in npDVR after high-order finite-difference approximation of the radial part of the kinetic energy operator on a quasiuniform grid. Such reduction permits us to use efficient computational algorithms for solving the special system of algebraic equations. We demonstrate the efficiency and flexibility of the computational scheme by two examples. It is three-dimensional (3D) atomic scattering confined in a strongly anisotropic waveguidelike trap and the system of four strongly coupled 2D Schrödinger-like equations describing the atomic collisions confined in a quasi-1D harmonic trap in the vicinity of magnetic Feshbach resonances. An example was also analyzed earlier with an alternative approach based on the expansion of the desired wave function over the harmonic oscillator basis [17]. We give a comparison with the alternative approach [17] to demonstrate advantages of our computational scheme. The developed computational method can be extended to other multichannel scattering problems with nonseparable angular part. Such problems arise in the description of atomic and molecular collisions in confined geometry of optical and electromagnetic traps of different configuration. The method permits us to treat the effects of spin and spin-orbit couplings as well as the effects of anisotropy in the interparticle interactions and in the interaction with the traps.

II. DESCRIPTION OF COMPUTATIONAL METHOD

A. Formulation of the problem: Scattering in confined geometry of atomic traps

The problem of multichannel scattering with a nonseparable angular part arises in ultracold atomic collisions confined by a harmonic waveguidelike trap [6]. Particularly, a challenging computational problem is to describe the scattering in the vicinity of Feshbach resonances [7,8]. In a general case,

*saeidian@iasbs.ac.ir

†melezhik@theor.jinr.ru

including the resonant scattering, the problem is to integrate the system of 3D Schrödinger-like equations,

$$\left(\left[-\frac{\hbar^2}{2\mu}\triangle_{\mathbf{r}}+\frac{1}{2}\mu\left(\omega_x^2x^2+\omega_y^2y^2\right)\right]\hat{I}+\hat{V}(r)\right)|\psi(\mathbf{r})\rangle = E|\psi(\mathbf{r})\rangle, \quad (1)$$

strongly coupled by the matrix of effective interatomic potential $\hat{V}(r)$ ($\hat{I}$ is the unit matrix here) and to find the wave function,

$$|\psi(\mathbf{r})\rangle=\sum_{\alpha}\psi_{\alpha}(\mathbf{r})|\alpha\rangle,\ \ \alpha=\{e,c=1\ldots\},$$

satisfying the scattering asymptotic,

$$\psi_e(\mathbf{r})=(e^{ik_0z}+f_e e^{ik_0|z|})\Phi_0(x,y),\quad \psi_c(\mathbf{r})\to 0, \quad (2)$$

at $|z|\to+\infty$ for the fixed collision energy E, where $\mathbf{r}=(x,y,z)=(\rho\cos\phi,\rho\sin\phi,z)=(r\sin\theta\cos\phi,r\sin\theta\sin\phi,r\cos\theta)$ is the relative variable between the colliding atoms. Here, $f_e(E)$ is the desired scattering amplitude, $\Phi_0(x,y)$ is the wave function of the ground state of the 2D harmonic oscillator $\frac{1}{2}\mu(\omega_x^2x^2+\omega_y^2y^2)$ describing interaction of the atoms with the confining trap, and $k_0=\sqrt{2\mu(E-\hbar\omega_\perp)}/\hbar=\sqrt{2\mu E_\parallel}/\hbar$ is the relative momentum of two atoms in the open channel "e," where $\omega_\perp=(\omega_x+\omega_y)/2$ and μ is the reduced mass of two colliding atoms.

Here, we consider two models for interatomic interaction. It is a scalar Gaussian potential,

$$V(r)=-V_0\exp\left\{-\left(\frac{r}{\bar{a}}\right)^2\right\}, \quad (3)$$

permitting analytic calculation of the matrix elements $\int\int\Phi_{n_x}(x)\Phi_{n_y}(y)V(x,y,z)\Phi_{n'_x}(x)\Phi_{n'_y}(y)dxdy$ in the "oscillator representation" being used in [17] for the desired wave function in (1) and (2),

$$\psi(\mathbf{r})=\sum_{n_x=1}^{N_x}\sum_{n_y=1}^{N_y}\chi_{n_xn_y}(z)\Phi_{2n_x-2}(x)\Phi_{2n_y-2}(y), \quad (4)$$

which is represented in the form of expansion over the product states Φ_{n_i} of the 1D harmonic oscillator. The summation over α is eliminated here ($\alpha=e$).

A four-channel tensorial potential $\hat{V}(r)$ is being used in [7] to describe three lowest magnetic Feshbach resonances in Cs [18]. Some of these resonances have been used in experimental investigation of the Cs confinement-induced resonances in anisotropic waveguidelike traps [19]. Following [7,18], we define $\hat{V}(r)$ as

$$\hat{V}(r)=\begin{pmatrix}-V_e & \hbar\bar{\Omega}_1 & \hbar\bar{\Omega}_2 & \hbar\bar{\Omega}_3\\ \hbar\bar{\Omega}_1 & -V_1(B) & 0 & 0\\ \hbar\bar{\Omega}_2 & 0 & -V_2(B) & 0\\ \hbar\bar{\Omega}_3 & 0 & 0 & -V_3(B)\end{pmatrix}\quad r<\bar{a}$$

$$=\begin{pmatrix}0&0&0&0\\0&\infty&0&0\\0&0&\infty&0\\0&0&0&\infty\end{pmatrix}\quad r>\bar{a}, \quad (5)$$

where $\bar{a}=4\pi\Gamma(1/4)^{-2}R_{vdW}$, R_{vdW} is the van der Waals tail of the interatomic interaction, $V_c(B)=V_c+\delta\mu(B-B_c)$, and the off-diagonal terms $\hbar\bar{\Omega}_c$ are defined by the formula

$$\left(\frac{\Gamma_c}{V_c}\right)^{1/2}=\frac{2\hbar\bar{\Omega}_c}{V_e-V_c},$$

where Γ_c is the Feshbach coupling strength of the channel "c" [18]. This matrix describes the interatomic interaction of colliding atoms in the open channel ("entrance channel") $|e\rangle$ and the weakly bound molecules in the closed channels $|c\rangle$ near Feshbach resonances. For $r<\bar{a}$, the attractive potentials V_e and V_c in the square-well form can support multiple molecular states and the parameters $\hbar\bar{\Omega}_c$ induce Feshbach couplings between the channels [18]. The range $\bar{a}$ of the potential action is chosen according to the range of the interatomic interaction determined by the van der Waals tail between atoms. For $r>\bar{a}$, entrance- and closed- channel thresholds are set to be $E=0$ and $E=+\infty$, respectively (see Fig. 1 in Ref. [18]). In the diagonal element V_{cc} the shift of the channel threshold $\delta\mu_c(B-B_c)$ is defined by interaction with the external magnetic field B. The relative magnetic moment $\delta\mu_c$ and B_c define the magnetic Feshbach resonances in the closed channels [18].

Note that, in the presence of an anisotropic harmonic trap ($\omega_x\neq\omega_y$), the problem (1) and (2) becomes nonseparable in 3D space $\{\rho,z,\phi\}$. To resolve the problem we have to integrate the 3D Schrödinger-like equation (1) [for the scalar potential (3)], or the system of equations [for the tensorial potential (5)]. In an isotropic trap ($\omega_x=\omega_y$) the problem admits separation of the angle ϕ and reduction to the 2D case. In free space ($\omega_x=\omega_y=0$) the angular part separates and the problem reduces to one [in the case of scalar potential (3)] or four [in the case of tensorial potential (5)] coupled radial equations. The last case was considered in [18]. The choice of the potential $\hat{V}(r)$ in the form (5) permitted the authors of the work [18] to construct an analytic model for describing Feshbach resonances in free space ($\omega_x=\omega_y=0$). However, to develop an efficient computational scheme for integration of the problem (1) and (2) in a confining trap ($\omega_x\neq0,\omega_y\neq0$) is a challenging task due to sharp jumps at $r=\bar{a}$ in the diagonal terms $V_{\alpha\alpha}(r)$ chosen in the form of a square-well potential.

B. Nondirect product DVR over angular variables

First, we discretize the problem (1) and (2) over angular variables θ and ϕ by applying the npDVR [12–16]. In this approach the desired wave function $|\psi(r,\theta,\phi)\rangle$ is expanded in the basis

$$f_j(\Omega)=\sum_{\nu=1}^{N}\bar{Y}_\nu(\Omega)[Y^{-1}]_{\nu j}, \quad (6)$$

which is orthogonal and complete on the 2D angular grid $\Omega_j=(\theta_{j_\theta},\phi_{j_\phi})$, so that

$$|\psi(r,\theta,\phi)\rangle=\frac{1}{r}\sum_{\alpha}\sum_{j=1}^{N}f_j(\Omega)u_j^{\alpha}(r)|\alpha\rangle. \quad (7)$$

Here N_θ and N_ϕ are the number of grid points θ_{j_θ} and ϕ_{j_ϕ} over the θ and ϕ variables respectively: $j_\theta=1,2,\ldots N_\theta$ and $j_\phi=1,2,\ldots N_\phi$. They define the total number $N=N_\theta\times N_\phi$ of grid points in the 2D angular subspace $\Omega=(\theta,\phi)$ and the number of basis functions (6) being used. The index $j=N_\phi\times$

TABLE I. The selected orthogonal basis $\bar{Y}_{lm}$ for $N_\theta = 9$ and $N_\phi = 5$.

	$m \longrightarrow$					
	$-\frac{N_\Phi-1}{2}$				$\frac{N_\Phi-1}{2}$	
$l = N_\theta - 1 + \frac{N_\phi-1}{2}$	$\bar{Y}_{10,-2}$				$\bar{Y}_{10,+2}$	
	$\bar{Y}_{9,-2}$	$\bar{Y}_{9,-1}$		$\bar{Y}_{9,+1}$	$\bar{Y}_{9,+2}$	
$l = N_\theta - 1$	$\bar{Y}_{8,-2}$	$\bar{Y}_{8,-1}$	$\bar{Y}_{8,0}$	$\bar{Y}_{8,+1}$	$\bar{Y}_{8,+2}$	
	$\bar{Y}_{7,-2}$	$\bar{Y}_{7,-1}$	$\bar{Y}_{7,0}$	$\bar{Y}_{7,+1}$	$\bar{Y}_{7,+2}$	
	$\bar{Y}_{6,-2}$	$\bar{Y}_{6,-1}$	$\bar{Y}_{6,0}$	$\bar{Y}_{6,+1}$	$\bar{Y}_{6,+2}$	
	$\bar{Y}_{5,-2}$	$\bar{Y}_{5,-1}$	$\bar{Y}_{5,0}$	$\bar{Y}_{5,+1}$	$\bar{Y}_{5,+2}$	
	$\bar{Y}_{4,-2}$	$\bar{Y}_{4,-1}$	$\bar{Y}_{4,0}$	$\bar{Y}_{4,+1}$	$\bar{Y}_{4,+2}$	$\uparrow$ l
	$\bar{Y}_{3,-2}$	$\bar{Y}_{3,-1}$	$\bar{Y}_{3,0}$	$\bar{Y}_{3,+1}$	$\bar{Y}_{3,+2}$	
	$\bar{Y}_{2,-2}$	$\bar{Y}_{2,-1}$	$\bar{Y}_{2,0}$	$\bar{Y}_{2,+1}$		
		$\bar{Y}_{1,-1}$	$\bar{Y}_{1,0}$	$\bar{Y}_{1,+1}$		
$l = 0$			$\bar{Y}_{0,0}$			

$(j_\theta - 1) + j_\phi$ represents here the twofold index $j = (j_\theta, j_\phi)$ and the summation over j is

$$\sum_{j=1}^{N} = \sum_{j_\theta=1}^{N_\theta} \sum_{j_\phi=1}^{N_\phi}. \tag{8}$$

The $N \times N$ matrix $\hat{Y}^{-1}$ is the inverse of the matrix $\hat{Y}$ defined as $Y_{j\nu} = \sqrt{\lambda_j}\bar{Y}_\nu(\Omega_j)$, with $\lambda_j = (2\pi\lambda'_{j_\theta})/N_\phi$ and λ'_{j_θ} being the weights of the Gaussian quadrature over θ. The angular grid points θ_{j_θ} and ϕ_{j_ϕ} are defined as the zeros of the Legendre polynomial $P_{N_\theta}(\cos\theta)$ and $\phi_{j_\phi} = 2\pi j_\phi/N_\phi$, respectively. The symbol ν represents the twofold index $\nu = (l,m)$ and the summation over ν is equivalent to (see Table I)

$$\sum_{\nu=1}^{N} = \sum_{m=-(N_\phi-1)/2}^{(N_\phi-1)/2} \sum_{l=|m|}^{|m|+N_\theta-1}. \tag{9}$$

The polynomials $\bar{Y}_\nu(\Omega)$ are chosen as

$$\bar{Y}_\nu(\Omega) = \bar{Y}_{lm}(\Omega) = e^{im\phi} \sum_{l'} d_l^{l'} P_{l'}^m(\theta), \tag{10}$$

where $d_l^{l'} = \delta_{ll'}$ holds, thus $\bar{Y}_\nu(\Omega)$ coincide with the usual spherical harmonics $Y_\nu(\Omega)$, except for $l \geqslant N_\theta$, so that the orthogonality relation remains

$$\begin{aligned} \langle \bar{Y}_\nu | \bar{Y}_{\nu'} \rangle &= \int \bar{Y}_\nu{}^*(\Omega)\bar{Y}_{\nu'}(\Omega)d\Omega \\ &\approx \sum_{j=1}^{N} \lambda_j Y_\nu^*(\Omega_j)Y_{\nu'}(\Omega_j) = \delta_{\nu\nu'}. \end{aligned} \tag{11}$$

However, for $l \geqslant N_\theta$ (see Table I), $Y_\nu(\Omega)$ have to be orthogonalized. We denote the set of orthogonal bases as $\bar{Y}_{lm}(\Omega)$. First, for $l = N_\theta$ we make a polynomial orthogonal to the ones of lower l value,

$$\widetilde{Y}_{lm}(\Omega) = Y_{lm}(\Omega) - \sum_{l'=|m|}^{l-1} \langle Y_{lm} | \bar{Y}_{l'm} \rangle \bar{Y}_{l'm}(\Omega), \tag{12}$$

and, we make it normalized,

$$\bar{Y}_{lm}(\Omega) = \frac{\widetilde{Y}_{lm}(\Omega)}{\langle \widetilde{Y}_{lm} | \widetilde{Y}_{lm} \rangle}. \tag{13}$$

Then, we perform the above procedure iteratively in order to obtain $\bar{Y}_{lm}(\Omega)$ for the next values of l. In this way, the above orthogonalization Gramm-Schmidt procedure leads to the basis (6) which is orthonormal and complete on the grid Ω_j for any chosen N.

By substituting expansion (7) into Eq. (1) and performing the scale transformation $r \to r/\bar{a}$, $E \to E/E_0$, $V \to V/E_0$, and $\omega \to \omega/\omega_0$ with $E_0 = \hbar^2/\mu\bar{a}^2$ and $\omega_0 = E_0/\hbar$, we reach a system of rescaled Schrödinger-like coupled equations with respect to the unknown vector $\mathbf{u}(r) = \{\sqrt{\lambda_j}u_j^\alpha(r)\}$,

$$(\hat{T}(r) + \hat{W}(r) + \hat{V}(r))\mathbf{u}(r) = E\mathbf{u}(r), \tag{14}$$

where

$$T_{jj'}^{\alpha\alpha'} = -\frac{1}{2}\left[\delta_{jj'}\frac{d^2}{dr^2} - \frac{1}{r^2}\sum_{\nu=1}^{N} Y_{j\nu} l(l+1)[Y^{-1}]_{\nu j'}\right]\delta_{\alpha\alpha'}, \tag{15}$$

$$W_{jj'}^{\alpha\alpha'} = \tfrac{1}{2}\left(\omega_x^2 x_j^2 + \omega_y^2 y_j^2\right)\delta_{jj'}\delta_{\alpha\alpha'}, \tag{16}$$

$$V_{jj'}^{\alpha\alpha'} = V_{\alpha\alpha'}(r)\delta_{jj'}. \tag{17}$$

Here $x_j = r\sin\theta_j\cos\phi_j$, $y_j = r\sin\theta_j\sin\phi_j$ and the elements $u_j^\alpha(r)$ of the vector $\mathbf{u}(r)$ coincide with the values $r\psi_\alpha(r,\Omega_j)$ of the desired wave function on the grid points Ω_j, $j = 1,\ldots,N$, $\alpha = e$ for (3) and $\alpha = \{e,c\}$ for (5).

Thus, by using the npDVR we transform the initial scattering problem (1) and (2) to the system of the Schrödinger-like coupled equations (14) with the following asymptotic:

$$u_j^e(r) = r(e^{ik_0 z_j} + f_e e^{ik_0|z_j|})\Phi_0(x_j,y_j), \quad u_j^c(r) = 0 \tag{18}$$

at $|z_j| = |r\cos\theta_j| \to +\infty$ and

$$u_j^\alpha(r) = 0, \tag{19}$$

at $r = 0$, which follows from the finiteness of the desired wave function $\psi_\alpha(\mathbf{r})$ ($\alpha = \{e,c\}$) at $r \to 0$.

C. Boundary conditions: Reduction of scattering problem to a boundary-value problem

The problem (14)–(19) is defined on the semiaxis $r \in [0,+\infty)$ which we replace by the interval $[0,r_m]$. The right edge of the interval r_m and any neighbor point r_{m-1} to the left of the edge must be chosen in such a way that some of the points $z_j^m = r_m\cos\theta_j$ and $z_j^{m-1} = r_{m-1}\cos\theta_j$ (say, for $j_\theta \leqslant j_m$ and for $j_\theta \geqslant N_\theta - j_m + 1$, where j_m is a constant) fall into the asymptotic region $|z_j^m| = |r_m\cos\theta_j| \to +\infty$ where the wave function $u_j^e(r)$ satisfies the asymptotic formulas (18) (see Fig. 1).

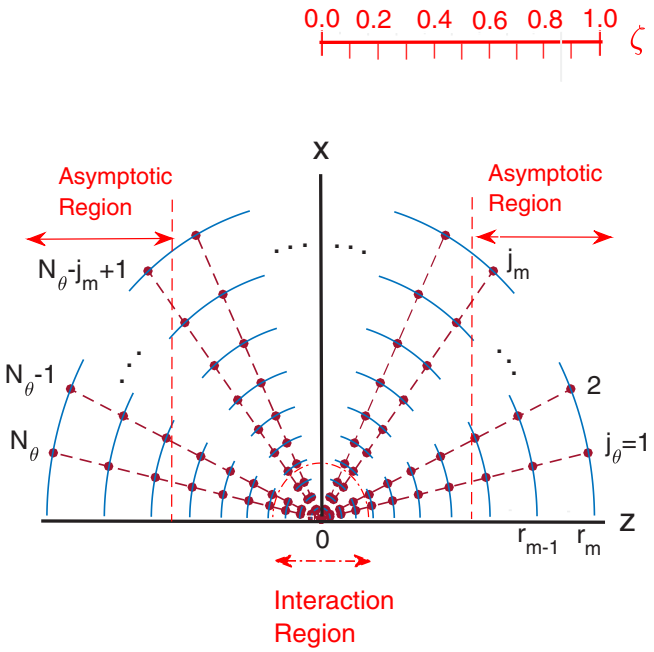

FIG. 1. The schematic figure of the grid points in x-z plane. The up horizontal axis shows the corresponding values of ζ.

By using two Eqs. (18) at the points r_m and r_{m-1} we eliminate the unknown amplitude f_e and construct the two-point boundary condition at the right edge of the interval $[0,r_m]$,

$$u_j^e(r_m) - u_j^e(r_{m-1})e^{ik_0(|z_j^m|-|z_j^{m-1}|)}\frac{r_m\Phi_0(x_j^m,y_j^m)}{r_{m-1}\Phi_0(x_j^{m-1},y_j^{m-1})}$$
$$= r_m\{e^{ik_0z_j^m} - e^{ik_0(z_j^{m-1}-|z_j^{m-1}|+|z_j^m|)}\}\Phi_0(x_j^m,y_j^m)$$
$$(\text{if } j_\theta \leqslant j_m \text{ or } j_\theta \geqslant N_\theta - j_m + 1),$$
$$u_j^e(r_m) = 0(\text{if } j_m < j_\theta < N_\theta - j_m + 1), \quad u_j^c(r_m) = 0, \tag{20}$$

where $x_j^m = r_m\sin\theta_j\cos\phi_j$ and $y_j^m = r_m\sin\theta_j\sin\phi_j$.

Thus, the initial scattering problem (1) and (2) is reduced to the boundary-value problem for the system of ordinary differential equations of second order (14) with the boundary conditions (19) and (20) which do not contain the unknown scattering amplitude f_e. After integration of the problem (14), (19), and (20) one can find the scattering amplitude f_e by mapping the calculated wave function $\psi_\alpha(r,\Omega_j)$ at the points $|z_j^m| = |r_m\cos\theta_j| \to +\infty$ with the asymptotic boundary condition (18).

To integrate the boundary-value problem (14), (19), and (20) one can apply efficient algorithms. By using the high-order (sixth-order) finite-difference approximation for the radial derivatives on a quasiuniform grid we arrive at a system of algebraic equations with block-band structure which can be solved by the LU decomposition [20] or the sweep (also known as the Thomas algorithm [21]) method [22], which are very efficient in terms of speed and memory requirements.

D. High-order finite-difference approximation over radial variable

We solve the system of Eqs. (14) on a quasiuniform radial grid [13]

$$r_n = r_m\frac{e^{\gamma\zeta_n}-1}{e^\gamma - 1}, \quad n = 1,2,\ldots,N_r \tag{21}$$

of N_r grid points $\{r_n\}$ defined by mapping $r_n \in [0,r_m](r_m \to +\infty)$ onto the uniform grid $\zeta_n \in [0,1]$ with the equidistant distribution $\zeta_n - \zeta_{n-1} = 1/N_r$. One can achieve a suitable distribution of the grid points for a specific interatomic and confining potential by varying N_r and the parameter $\gamma > 0$. After the seven-point finite-difference approximation (sixth-order approximation) of the derivatives in the system of ordinary differential equations (14), the boundary-value problem (14), (19), and (20) is reduced to the system of N_r matrix equations,

$$\sum_{p=1}^{3} R_{n-p}\hat{I}\mathbf{u}_{n-p} + (\hat{A}_n + \hat{W}_n + \hat{V}_n - E\hat{I})\mathbf{u}_n$$
$$+ \sum_{p=1}^{3} R_{n+p}\hat{I}\mathbf{u}_{n+p} = 0, (n = 1,2,\ldots,N_r - 3),$$
$$\times\mathbf{u}_n + \hat{B}_n\mathbf{u}_{n-1} = \mathbf{g}_n \quad (n = N_r - 2, N_r - 1, N_r). \tag{22}$$

Here, the matrix of coefficients of the system of algebraic equations (22) has a block-band structure with the width of the band equal to $7\times N$ [for scalar potential (3)] or $7\times 4\times N$ [for tensorial potential (5)]. The definition of the $4N\times 4N$ matrices $V_{jj'}^{\alpha\alpha'}(r_n) = V_j^{\alpha\alpha'}(r_n)\delta_{jj'}$, $W_{jj'}^{\alpha\alpha'}(r_n) = W_j^\alpha(r_n)\delta_{jj'}\delta_{\alpha\alpha'}$, and the angular part $A_{jj'}^{\alpha\alpha'}(r_n) = A_{jj'}^\alpha\delta_{\alpha\alpha'}$ of the matrix of the kinetic energy operator $\hat{T}(r)$ are given by Eqs. (15)–(17). The coefficients R_n arise due to sixth-order finite-difference approximation of the radial part of the kinetic energy operator $\hat{T}(r)$ (15). The unknown vector $\mathbf{u}_n$ in (22) defines the desired wave function $\psi_\alpha(r_n,\Omega_j) = u_j^\alpha(r_n)/r_n$ on the 3D grid $\{r_n,\Omega_j\}$, where $n = 1,2,\ldots,N_r$; $j = 1,2,\ldots,N$ and $\alpha = e$ [for (3)] or $\alpha = \{e,c\}$ [for (5)]. In the first three equations of the system (22), the functions u_{-3}, u_{-2}, u_{-1},

TABLE II. The run time τ of our code for calculation of $T(N,N_r)$ for $N = 30$ (a) and $N_r = 1.0\times 10^5$ (b). The code has been run on a 3.4-GHz CPU.

$N_r/10^5$ (a)	$\tau(s)$	N (b)	$\tau(s)$
0.2	3.5×10^3	2	4.8×10^0
0.4	4.8×10^3	3	1.4×10^1
0.6	9.1×10^3	4	2.9×10^1
0.8	9.7×10^3	5	8.9×10^1
1.0	1.5×10^4	6	1.1×10^2
1.5	2.6×10^4	8	3.0×10^2
2.0	2.9×10^4	10	5.5×10^2
3.0	5.2×10^4	12	8.6×10^2
4.0	6.9×10^4	15	2.6×10^3
5.0	8.7×10^4	20	5.9×10^3
7.5	1.3×10^5	25	9.9×10^3
10.0	1.7×10^5	30	1.5×10^4

TABLE III. The convergence of the expansion (7) with respect to $N{=}N_\theta$, N_r, and r_m for fixed $N_\phi{=}1$, where $\Delta T(N) = T(N+2) - T(N)$. Calculations were performed for the scattering on the scalar potential (3) in isotropic trap with $\omega_x = \omega_y = 0.02$.

	$r_m = 60$				$r_m = 65$	$r_m = 70$
	$N_r = 130$		$N_r = 200$	$N_r = 400$	$N_r = 400$	$N_r = 400$
$N = N_\theta$	T	$\Delta T(N)$	T	T	T	T
13	0.044 495	0.569 612				
15	0.614 207	0.173 223				
17	0.440 984	0.026 273				
19	0.414 711	0.005 976				
21	0.408 735	0.001 311	0.409 657	0.410 674	0.412 752	0.413 557
23	0.407 424	0.000 157	0.407 665	0.407 947	0.408 539	0.408 740
25	0.407 267	0.000 153	0.407 272	0.407 334	0.407 468	0.407 527
27	0.407 114	0.000 013	0.407 158	0.407 189	0.407 222	0.407 245

and u_0 are omitted by using the left-side boundary condition (19): $u_0 = 0$ and $u_{-n} = -u_n$. The last three equations with $n = N_r - 2$, $N_r - 1$, and N_r in the system represent the boundary condition (20), where the matrix $B^\alpha_j(r_n)\delta_{jj'}\delta_{\alpha\alpha'}$ and the vector $\mathbf{g}_n = \{g^\alpha_j(r_n)\}$ are given by Eq. (20).

We solve this boundary-value problem by using the fast implicit matrix algorithm [6] (see Appendix B therein) which is based on the LU decomposition approach [20] or the sweep method [22,23] and takes into consideration the block-band structure of matrix of coefficients of the system (22). It leads to high efficiency of the algorithm in speed and memory: exclusion of the calculation of zero elements, which make up the bulk of the matrix of coefficients in (22), dramatically decreases the required computer memory and leads to proportionality of the computational time to the number of radial grid points N_r. Table II shows the run time τ of our code for several values of N_r and N. The linear dependence of τ on N_r is clear. At that, τ is proportional to N^3 according to the theory of the matrix sweeping method (the block-elimination method) [23]. Therefore, application of the matrix sweeping method is particularly efficient if it is possible to keep $N \ll N_r$ during computations. This is a case considered in Sec. IV B.

III. NUMERICAL EXAMPLES

To demonstrate the computational efficiency of the method we consider here two numerical examples with the scalar potential (3), leading to 3D scattering in an anisotropic atomic waveguide, and tensorial interatomic interaction (5), which models four-channel 2D scattering confined in an isotropic atomic waveguide in the vicinity of a Feshbach resonance in Cs [7].

A. Scalar interatomic interaction (3)

With the interaction potential (3) we have investigated the convergence of our computational scheme with respect to $N, N_r \to +\infty$ and $r_m \to +\infty$ by using as an example calculation of a measurable scattering parameter the transmission $T = |1 + f_e|^2$. Investigation is carried out in two stages. First, we analyze the convergence of the method for the isotropic waveguidelike trap with $\omega_x = \omega_y = 0.02$, $E_\parallel = 5 \times 10^{-5}$, and $V_0 = 0.495$. At that, the system has cylindrical symmetry which leads to separation of the ϕ variable. The problem becomes a 2D one and $N = N_\theta$. The results of calculation of the transmission $T(N,N_r,r_m)$ are given in Table III. This investigation demonstrates good convergence of the npDVR here: to get the accuracy of the order $\sim 10^{-4}$ it needs to keep $N \sim 23$–25 in the expansion (7). To keep the same order of accuracy due to radial grid approximation it is enough to fix $N_r = 130$ and $r_m = 60$ at $N \gtrsim 25$.

Next, we apply the method to the 3D case with an anisotropic trap ($\omega_x/\omega_y \neq 1$) leading to strong nonseparability of the angular part. In Table IV the results of calculation of the transmission $T(N_\phi)$ are given for $\omega_x/\omega_y = 4/3$, 1.5, and 2 with N_θ, N_r, and r_m fixed in the previous stage performed for the isotropic case. This investigation demonstrates rather fast convergence of the method even for strong anisotropy of the trap: at $N_\phi = 9$ the reached accuracy varies from 2×10^{-5} to 10^{-3} with increasing the anisotropy of the trap from $\omega_x/\omega_y = 4/3$ up to 2.

We have also calculated the transmission $T(N)$ for the above-considered anisotropic cases with the expansion (4) over the product states Φ_{n_i} of the 1D harmonic oscillator. This alternative approach was used in [17]. It gives diagonal representation for atom-trap interaction $W_{jj'} = 1/2(\omega_x + \omega_y)\delta_{jj'}$ but the atom-atom interaction (3) is off diagonal in contrast to npDVR. However, the chosen Gaussian model (3) for atom-atom interaction permits the analytic computation of the corresponding matrix elements. This advantage is lost for other forms of the interaction. The convergence of this

TABLE IV. The convergence of the expansion (7) with respect to N_ϕ for fixed $N_\theta = 25$, where $\Delta T(N_\phi) = T(N_\phi + 2) - T(N_\phi)$. Calculations were performed for the scattering on the scalar potential (3) in anisotropic trap with $\omega_x = 0.02$ on the radial grid with $N_r = 130$ and $r_m = 60$.

	$\frac{\omega_x}{\omega_y} = \frac{4}{3}$		$\frac{\omega_x}{\omega_y} = 1.5$		$\frac{\omega_x}{\omega_y} = 2$	
N_ϕ	T	$\Delta\, T(N_\phi)$	T	$\Delta\, T(N_\phi)$	T	$\Delta\, T(N_\phi)$
1	0.141 75	0.174 46	0.1549	0.1253	0.1721	0.0864
3	0.316 21	0.152 75	0.2802	0.2057	0.2585	0.2398
5	0.468 96	0.004 43	0.4859	0.0117	0.4983	0.0413
7	0.473 39	0.000 92	0.4976	0.0037	0.5396	0.0336
9	0.474 31	0.000 02	0.5013	0.0001	0.5732	0.0024
11	0.474 33		0.5014		0.5756	

TABLE V. The convergence of the expansion (4) with respect to $N = N_x \times N_y$, where $\Delta T(N) = T(N_x \times N_y) - T[(N_x + 1) \times (N_y + 1)]$. Calculations were performed for scattering on the scalar potential (3) in anisotropic trap with $\omega_x = 0.02$ on the radial grid with $N_r = 130$ and $r_m = 60$.

	$\frac{\omega_x}{\omega_y} = \frac{4}{3}$		$\frac{\omega_x}{\omega_y} = 1.5$		$\frac{\omega_x}{\omega_y} = 2$	
N	T	$\Delta T(N)$	T	$\Delta T(N)$	T	$\Delta T(N)$
4	0.5460	0.0098	0.5734	0.0094	0.6425	0.0086
9	0.5362	0.0073	0.5640	0.0071	0.6339	0.0064
16	0.5289	0.0057	0.5569	0.0056	0.6275	0.0052
25	0.5232	0.0048	0.5513	0.0047	0.6223	0.0044
36	0.5184	0.0040	0.5466	0.0040	0.6179	0.0037
49	0.5144	0.0035	0.5426	0.0035	0.6142	0.0033
64	0.5109	0.0030	0.5391	0.0030	0.6109	0.0028
81	0.5079	0.0027	0.5361	0.0027	0.6081	0.0026
100	0.5052	0.0024	0.5334	0.0024	0.6055	0.0024
121	0.5028	0.0022	0.5310	0.0022	0.6031	0.0021
144	0.5006	0.0019	0.5288	0.0019	0.6010	0.0019
169	0.4987	0.0017	0.5269	0.0019	0.5991	0.0018
196	0.4970		0.5251		0.5973	

alternative approach is demonstrated in Table V. It is shown that already the first four terms in (4) give a rather accurate approximation of the transmission T (with the error of the order $\sim$0.07). However, further increase of the number N of the basis function in the expansion (4) gives very slow convergence: at maximal $N = 196$ the accuracy of the order $\sim(2\text{–}3) \times 10^{-2}$ is only achieved even for weak trap anisotropy ($\omega_x/\omega_y = 4/3$) in contrast to our approach. Note the specific peculiarity of the expansion (4): the convergence over N has weak dependence on the trap anisotropy.

B. Tensorial resonant interatomic interaction (5)

We have also applied the method to integration of the problem (1) and (2) with the tensorial potential (5). This potential was suggested in [18] for analytical description of Feshbach resonances in Cs gas in free space where the angular part was separated and the problem permitted an analytical solution. However, including into consideration the atom-trap interaction makes the problem (1) and (2) computationally extremely challenging even for an isotropic confining trap with $\omega_x/\omega_y = 1$. Actually, it demands simultaneous treatment of the sharp jumps of the diagonal terms $V_{\alpha\alpha}(r)$ (17) in the edge $\bar{a}$ of the action of the potential, numerous oscillations of the wave function at $r \lesssim \bar{a}$ caused by the molecular states in the region of interatomic interaction, and strong resonant coupling of open entrance channel ''e" with closed channels "c."

The parameters of the confining trap $\omega_x = \omega_y = \omega_\perp$ were chosen in a range of variation of $\omega_\perp$ close to the experimental values of the trap frequencies $\omega_\perp \sim 2\pi \times 14.5$ kHz [19] and the parameters of the interaction potential (5) were fixed in our work [7] to reproduce the positions and widths of the s, d, and f resonances for Cs in free space. In the case of isotropic waveguide trap $\omega_x = \omega_y$, the problem (1) is reduced to the system of four coupled 2D Schrödinger-like equations: the ϕ variable is separated and the 2D polynomials (10) degenerate to the usual Legendre polynomials $P_l(\theta)$.

TABLE VI. The obtained values of the fitting parameters V_α in units of $10^{-3} E_0$ and $\delta\mu_c$ in units of the Bohr magneton μ_B for $N = 20$, $N_r = 1.0 \times 10^6$, and $r_m = 100\bar{a}$.

α	V_α	$\delta\mu_c$
1	7.565 843	2.2455
2	7.519 637	1.1520
3	7.519 637	1.5100
e	7.770 325	

We have integrated Eq. (1) for varying B and fixed longitudinal colliding energy $E_{||} = E - \hbar\omega_\perp = 1.0 \times 10^{-6} E_0 = 2.45 \times 10^{-14}$ eV $\to 0$ with $\Gamma_1/\hbar = 11.63$ MHz, $\Gamma_2/\hbar = 0.065$ MHz, $\Gamma_3/\hbar = 0.0042$ MHz, $B_1 = 19.7$ G, $B_2 = 48.0$ G, and $B_3 = 53.5$ G [18]. The parameters V_α and $\delta\mu_c$ in Table VI are obtained by fitting the calculated scattering length $a_s(B)$ (which can be extracted from the scattering amplitude f_e) in free space with the experimental data [18].

In Fig. 2 we present the calculated probability density distribution $|\psi_e(x,z)|^2$ in the vicinity of a d-wave Feshbach resonance (occurring at $B_{0,d} = 47.8$ G [18]) for $B = 47.9$ G. This resonance is developed as a peak at $r \lesssim \bar{a}$ in the plot of the probability density distribution with numerous oscillations over r (which is not clear in the figure), due to occurrence of quasimolecular states. In the asymptotic region $|z| \to +\infty$ we observe one oscillation of the entrance channel wave function $\psi_e(x,z)$ (2) with the period $2\pi/k_0 \to \infty$ defined by very small colliding energy $k_0 = \sqrt{2\mu E_{||}}/\hbar \to 0$.

Figure 3 illustrates the convergence of the method with respect to the number of grid points N over the angular variable on a typical example of calculating the T coefficient near s-wave Feshbach resonance (which occurs at $B_{0,s} = -11.16$ G [18]) for $B = 14.14$ G. It demonstrates rather fast convergence of the npDVR in the problem over the angular grid points

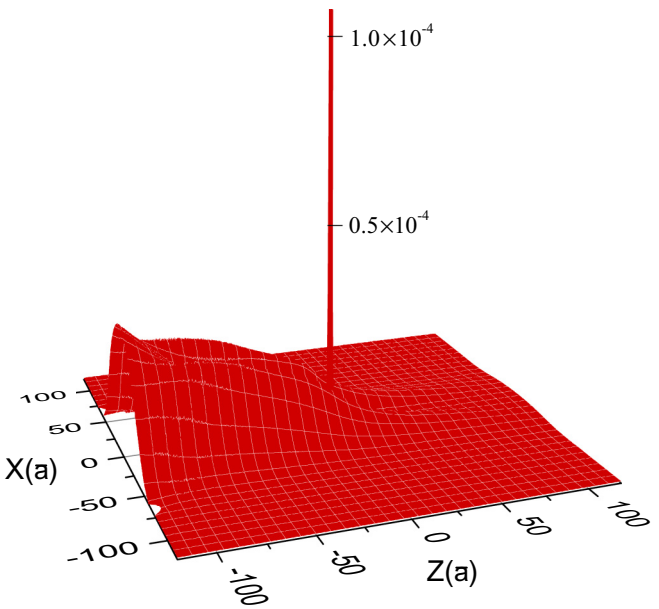

FIG. 2. The calculated probability density distribution $|\psi_e(x,z)|^2$ in the entrance channel "e" of the scattering problem (1) and (2) with the tensorial potential (5) for $B = 47.9$ G.

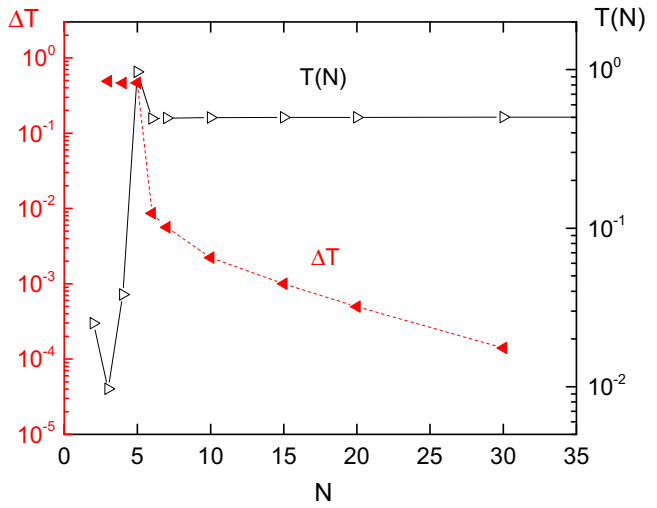

FIG. 3. The dependence of the transmission $T(N)$ and absolute error $\Delta T(N) = |T(N) - T(N = 40)|$ due to npDVR (7) on the number of angular grid points N. Calculations were performed for scattering on the tensorial potential (5) for $B = 14.14$ G, $N_r = 1.0 \times 10^6$, and $r_m = 100\bar{a}$.

despite the strong coupling over the angular variable provided by the atom-trap interaction potential $1/2\mu\omega_\perp^2 r^2 \sin^2\theta$ in the wide area of variation of the interatomic distance r. It is shown that for getting absolute accuracy on the level 10^{-3} it is enough to keep about $N = 10$ of terms in the expansion (7). Further computations with increasing N demonstrate monotonic convergence to a more accurate T coefficient. To reach the level of accuracy $\simeq 10^{-4}$ it needs to be increased up to $N \simeq 30$.

Figure 4 illustrates the scheme of convergence for $N_r \to \infty$. To keep absolute accuracy in the level $\simeq 10^{-4}$ we need to choose the rather big $N_r \simeq 10^6$ (see Fig. 4), corresponding to

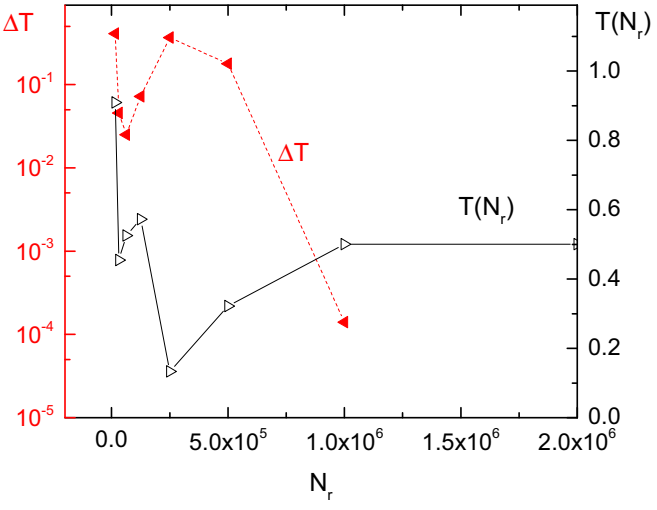

FIG. 4. The dependence of the transmission coefficient $T(N_r)$ and absolute error $\Delta T(N_r) = |T(N_r) - T(N_r = 2.0 \times 10^6)|$ due to finite-difference approximation of radial derivatives in (14) on the number of grid points N_r over radial variable r. Calculations were performed for scattering on the tensorial potential (5) for $N_\theta = 20$, $r_m = 100\bar{a}$, and $B = 14.14$ G.

the step $1/N_r = 10^{-6}$ of the equidistant grid over ζ in (21). So small a step is demanded for a good approximation of the oscillating behavior of the desired wave function in the region $r \lesssim \bar{a}$ (see Fig. 2) and the sharp jump of the potentials $V_{\alpha\alpha}(r)$ near the border $\bar{a}$ (see Table VI).

The rather routine procedure of choosing the range of integration r_m over r shows that to keep the accuracy at the same level $\simeq 10^{-4}$ we need to choose r_m rather large, $r_m \simeq 100\bar{a}$. This is a consequence of the long-range asymptotical behavior of the scattering wave function (2) with respect to $k_0 r_m \cos\theta_j \to +\infty$ in the zero-energy limit, $k_0 \to 0$, which is under consideration here.

IV. CONCLUSION

We have developed an efficient computational method based on the npDVR for multichannel scattering with a nonseparable angular part, confined in atomic traps. We reformulate the scattering problem for coupled 3D Schrödinger-like equations as a boundary-value problem for a system of algebraic equations with block-band structure of the well-defined matrix of coefficients which arises in npDVR after high-order finite-difference approximation of the radial part of the kinetic energy operator. Such a reduction permits us to apply here the computational algorithms efficient for speed and memory requirements. We demonstrate the efficiency and good convergence of the method for the 3D scattering confined in strongly anisotropic traps and the system of four coupled 2D Schrödinger-like equations which describes the atomic collisions confined in a waveguidelike isotropic harmonic trap in the vicinity of magnetic Feshbach resonances in Cs [18].

With this method the shifts and widths of the Cs and K Feshbach resonances in isotropic harmonic waveguides were calculated in our works [7,8] for the first time. The calculated shifts of the Cs Feshbach resonances (confinement-induced resonances) show excellent agreement with the experimental data [19] and with the simple estimate obtained in the pseudopotential approach for the positions of the confinement-induced resonances [24]. In the present work we give a detailed description of the method and its extension to the case of an anisotropic waveguidelike confining trap, i.e., to the case of multichannel scattering for coupled 3D Schrödinger-like equations. The formulas obtained here permit us to consider the effects of anisotropy in the interparticle interactions and in the interaction with the traps as well as the effects of spin and spin-orbit coupling. Such problems arise at a description of atomic and molecular collisions in confined geometry of optical and electromagnetic traps of different configurations. Application of the method to this kind of problem and to other actual multichannel scattering problems with nonseparable angular part looks very promising thanks to the fast convergence and the flexibility: there is no need for laborious calculations of the matrix elements with a change of the form of the interactions because any local interaction is diagonal in the npDVR.

ACKNOWLEDGMENT

The work was financially supported by the Ministry of Education and Science of the Russian Federation (Agreement No. 02.a003.21.0008).

[1] C. Chin, R. Grimm, P. S. Julienne, and E. Tiesinga, Rev. Mod. Phys. **82**, 1225 (2010).
[2] T. Köhler, K. Góral, and P. S. Julienne, Rev. Mod. Phys. **78**, 1311 (2006).
[3] V. S. Melezhik and C.-Y. Hu, Phys. Rev. Lett. **90**, 083202 (2003).
[4] B. Deb and L. You, Phys. Rev. A **64**, 022717 (2001).
[5] V. S. Melezhik, J. Comput. Phys. **92**, 67 (1991).
[6] S. Saeidian, V. S. Melezhik, and P. Schmelcher, Phys. Rev. A **77**, 042721 (2008).
[7] S. Saeidian, V. S. Melezhik, and P. Schmelcher, Phys. Rev. A **86**, 062713 (2012).
[8] S. Saeidian, V. S. Melezhik, and P. Schmelcher, J. Phys. B **48**, 155301 (2015).
[9] V. S. Melezhik, J. Phys.: Conf. Ser. **497**, 012027 (2014)
[10] S. Shadmehri, S. Saeidian, and V. S. Melezhik, Phys. Rev. A **93**, 063616 (2016).
[11] V. S. Melezhik and A. Negretti, Phys. Rev. A **94**, 022704 (2016).
[12] V. S. Melezhik, in *Atoms and Molecules in Strong External Fields*, edited by P. Schmelcher and W. Schweizer (Plenum, New York and London, 1998), p. 89.
[13] V. S. Melezhik, Phys. Lett. A **230**, 203 (1997).
[14] V. S. Melezhik and D. Baye, Phys. Rev. C **59**, 3232 (1999).
[15] V. S. Melezhik, in *Numerical Analysis and Applied Mathematics ICNAAM 2012: International Conference of Numerical Analysis and Applied Mathematics*, AIP Conf. Proc. No. 1479, edited by T. E. Simos, G. Psihoyios, C. Tsitouras, and Z. Anastassi (AIP, Melville, NY, 2012), p. 1200.
[16] V. S. Melezhik, EPJ Web Conf. **108**, 01008 (2016).
[17] V. S. Melezhik and P. Schmelcher, Phys. Rev. A **84**, 042712 (2011).
[18] A. D. Lange, K. Pilch, A. Prantner, F. Ferlaino, B. Engeser, H.-C. Nägerl, R. Grimm, and C. Chin, Phys. Rev. A **79**, 013622 (2009).
[19] E. Haller, M. J. Mark, R. Hart, J. G. Danzl, L. Reichsöllner, V. Melezhik, P. Schmelcher, and H. C. Nägerl, Phys. Rev. Lett. **104**, 153203 (2010)
[20] W. H. Press, S. A. Teukolsky, W. T. Vetterling, and B. P. Flannery, *Numerical Recipes* (Cambridge University Press, Cambridge, England, 1992), p. 34.
[21] G. N. Bruce, D. W. Peacemen, H. H. Rachford, Jr., and J. D. Rice, Trans. AIME **198**, 79 (1953).
[22] I. M. Gelfand and S. V. Fomin, *Calculus of Variations* (Dover, New York, 2000).
[23] A. A. Samarskii and E. S. Nikolaev, *Numerical Methods for Grid Equations* (Birkhäuser Verlag, Basel, 1989), Chap. 2.
[24] M. Olshanii, Phys. Rev. Lett. **81**, 938 (1998).